Polyoxometalates

DOI: 10.1002/anie.200903299

A Gadolinium-Bridged Polytungstoarsenate(III) Nanocluster: $[Gd_8As_{12}W_{124}O_{432}(H_2O)_{22}]^{60-}$**

Firasat Hussain, Franziska Conrad, and Greta R. Patzke**

Polyoxometalates (POMs: macromolecular oxoclusters of transition metals in high oxidation states)[1–3] are unmatched in terms of structural versatility and potential applications in for example medicine, catalysis, multifunctional materials, imaging, and bio- and nanotechnology.[4–16] Amongst the multitude of polyoxometalate structural motifs, the lanthanoid-containing POMs offer particularly interesting features, such as magnetism, luminescence, Lewis acid catalysis, and the development of magnetic resonance imaging (MRI) contrast agents from Gd-POMs.[17] The synthetic combination of a lacunary POM with highly basic oxygen atoms with large oxophilic lanthanoid cations is a powerful strategy to form molecular polyoxoanion complexes with a large number of metal centers or extended metal–oxygen frameworks.

Since the first lanthanoid-containing POMs were reported in 1971,[18] many other groups have been working on the development of such clusters (for example Pope, Müller, Francesconi, Yamase, Krebs, Gouzerh, Sécheresse, and Kortz; for a detailed survey, see the Supporting Information, Table S1).[19] The cerium-containing polyoxotungstoarsenate-(III), $[Ce_{16}As_{12}(H_2O)_{36}W_{148}O_{524}]^{76-}$ from Pope et al., still remains the largest polyoxotungstate known,[20] followed by the dimethyltin-containing W_{108} species published by one of us.[21] Herein, we present the lanthanoid-containing nanocluster $[Gd_8As_{12}W_{124}O_{432}(H_2O)_{22}]^{60-}$ (**1**) as the second-largest polyoxotungstate reported to date.

Even the largest polyoxotungstates are still considerably smaller in terms of metal centers than molybdenum-containing Keplerate POMs from Müller, which contain pentagonal $\{(Mo)Mo_5\}$ units.[22] Pentagonal units are considered to be of central importance for the construction of giant species with curvatures. Therefore, the isolation of large molecular polyoxotungstates with dimensions comparable to the Keplerate-type polyoxomolybdates remains an ongoing challenge; recently, Müller et al. reported a $\{W_{72}Mo_{60}\}$ structure that is the first polyoxotungstate of the thousands known that contains $\{(W)W_5\}$ units.[19l] The majority of the monosubstituted lanthanoid-containing POMs are constructed from Keggin-type fragments leading to the formation of one-dimensional chains, two-dimensional layers, or sandwich-type POMs.[14,19h–j] We thus systematically explored the reactivity of mid- and late lanthanoid ions with the dilacunary lone-pair-containing polyoxotungstate $[As_2W_{19}O_{67}(H_2O)]^{14-}$.[23–25]

$[As_2W_{19}O_{67}(H_2O)]^{14-}$, which is constructed from two $\{AsW_9O_{33}\}^{9-}$ subunits that are connected by a $\{WO_6\}$ octahedron, has a versatile isomerization behavior in the presence of alkali cations or at low pH values.[23–25] The combination of the $\{As_2W_{19}\}$ building block with lanthanoid ions in concentrated sodium-ion-containing solutions is thus likely to result in the formation of the long-sought-after large discrete polyoxotungstates, as indicated by recent work on Ln-POMs containing $\{AsW_9\}$ units.[25]

We obtained the first octanuclear gadolinium-containing tungstoarsenate(III), $[Gd_8As_{12}W_{124}O_{432}(H_2O)_{22}]^{60-}$ (**1**) with 124 tungsten centers (Figure 1). Moreover, compound **1** is

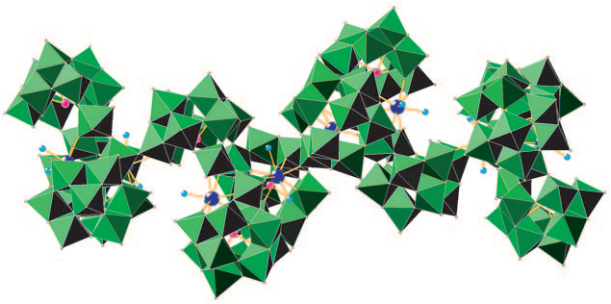

Figure 1. Polyhedron representation of $[Gd_8As_{12}W_{124}O_{432}(H_2O)_{22}]^{60-}$. W green, As pink, Gd blue, O red, H_2O cyan.

longer than other lanthanoid-containing polytungstates with more than 100 tungsten centers. Polyanion **1** was synthesized in a one-pot reaction starting from a 1:2 ratio of the dilacunary POM[23] $K_{14}[As_2W_{19}O_{67}(H_2O)]$ and $Gd(NO_3)_3{\cdot}6H_2O$ in 1 M NaOAc/CH_3COOH buffer at pH 4.7, and it was isolated as a mixed sodium–potassium–cesium salt with the empirical formula $Na_{35}K_{14}Cs_{11}[Gd_8As_{12}W_{124}O_{432}(H_2O)_{22}]{\cdot}n\,H_2O$ ($n \approx 123$). Compound **1** was also obtained from the reaction of the aforementioned starting materials in 0.5 M NaOAc/CH_3COOH buffer at pH 4.7, but in lower yield.

[*] Dr. F. Hussain, F. Conrad, Prof. G. R. Patzke
Institute of Inorganic Chemistry, University of Zurich
Winterthurerstrasse 190, 8057 Zurich (Switzerland)
Fax: (+41) 446-356-802
E-mail: firasat.hussain@aci.uzh.ch
greta.patzke@aci.uzh.ch

[**] This work was supported by the Swiss National Science Foundation (SNSF Professorship PP002-114711/1) and the University of Zurich. We thank Dr. B. Spingler, Institute of Inorganic Chemistry, University of Zurich, for helpful crystallographic discussions, and S. Weyeneth, Physics Institute, University of Zurich, for assistance with the magnetic measurements. We are grateful to Prof. A. Stemmer and R. Enning, Micro and Nano Science Platform, ETH Zurich, for help with AFM measurements. We thank Dr. R. Wepf, Electron Microscopy ETH Zurich, EMEZ, for Cryo-SEM investigations. The support of the Center for Microscopy and Image Analysis, University of Zurich, is gratefully acknowledged, and we thank Y. Zhou, UZH, for help with SEM measurements.

Supporting information for this article is available on the WWW under http://dx.doi.org/10.1002/anie.200903299.

This novel polyanion crystallizes in the triclinic space group $P\bar{1}$, and the crystallographic center of inversion leads to a nominal point group symmetry of C_i. Two identical subunits with the formula $\{Gd_4As_6W_{62}O_{216}(H_2O)_{11}\}^{30-}$ (**1a**) are related by the inversion center and thus constitute polyanion **1** (Figure 1). The subunit **1a** can be described as a dimer of two equally charged trimers: $[Gd_2As_3W_{31}O_{108}(H_2O)_6]^{15-}$ and $[Gd_2As_3W_{31}O_{108}(H_2O)_5]^{15-}$, which are linked through W31-O114-W32 and Gd1-O113-W37 bridges (Figure 2; W31–O114: 2.19 Å, W32–O114: 1.74 Å, Gd1–O113: 2.41 Å, W37–O113: 1.74 Å). The subunits **1a** are thus composed of six $\{B\text{-}\alpha\text{-}As^{III}W_9O_{33}\}$ fragments and distorted $\{Gd_2(H_2O)_6W_4O_9\}^{12+}$ and $\{Gd_2(H_2O)_5W_4O_9\}^{12+}$ subunits. Each trimer consists of three trilacunary $\{AsW_9O_{33}\}$ fragments that are linked through two $\{WO_6\}$ octahedra and two $\{WO_5(H_2O)\}$ octahedra or one $\{WO_5(H_2O)\}$ octahedron, respectively. This connectivity mode has only seldom been observed in POM structures; some examples include $[Ho_5(H_2O)_{16}(OH)_2As_6W_{64}O_{220}]^{25-}$, $[P_2W_{19}O_{69}(OH_2)]^{14-}$, and $[Si_2W_{23}O_{77}(OH)]^{9-}$.[19g,26,27] Each trimeric subunit of **1** contains two eight-coordinate gadolinium(III) ions with Gd–O bond lengths ranging from 2.214 to 2.467 Å. All of the gadolinium(III) ions are arranged in a linear fashion, and each of them is surrounded by two terminal aqua ligands. Bond valence sum (BVS) calculations[28] indicate that no oxygen atoms of the six $\{AsW_9O_{33}\}$ moieties in the $\{Gd_4As_6W_{62}O_{216}(H_2O)_{11}\}^{30-}$ subunit **1a** are protonated, and three terminal dihydroxo ligands were identified on three tungsten centers positioned in *trans* orientation. None of the W-O-W or Gd-O-W bridges are mono- or diprotonated so that the overall charge of **1** is −60, which is balanced by countercations in the solid state. As outlined above, **1** is a dimer of the dimeric building unit **1a**; this hierarchical arrangement renders **1** the longest polyoxotungstate known to date, with overall dimensions of about 4.8 nm. Polyanion **1** can therefore be described as a dimer of polyanions **1a** that are interconnected by terminal oxygen atoms of a $\{AsW_9O_{33}\}$ unit and the terminal oxygen atoms of Gd3 by two long Gd3-O203-W57 bridges.

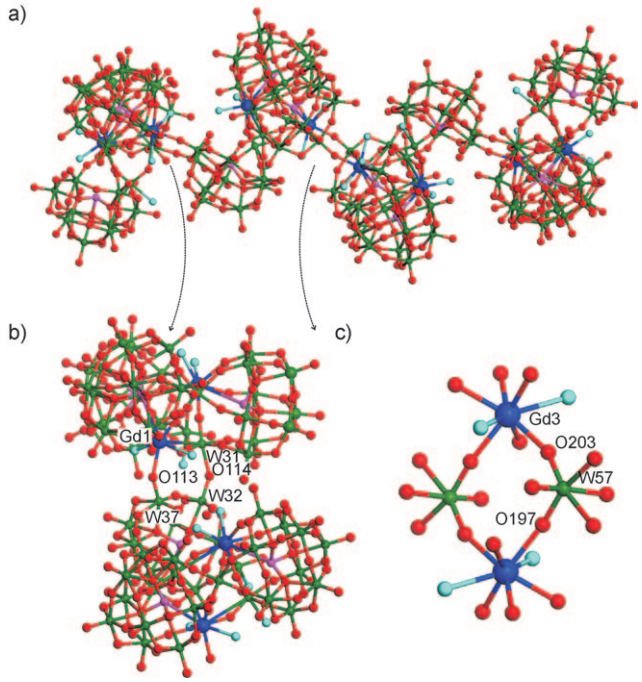

Figure 2. a) Ball-and-stick representation of the architecture of $[Gd_8As_{12}W_{124}O_{432}(H_2O)_{22}]^{60-}$ (**1**); b) asymmetric unit of the polyanion and c) core unit of the polyanion with Gd-O-W bridges. W green, As pink, Gd blue, O red, H_2O cyan.

The length of the bonds between the dimers suggests that **1** might break apart at this point of weakness in dilute solutions (cf. Figure 2: W57–O203 1.76 Å, Gd3–O203 2.33 Å, W57–O197 1.78 Å, Gd3–O197 2.33 Å). Generally, the analytical investigation of this problem is quite challenging; furthermore, initial attempts using ^{183}W NMR spectroscopy were unsuccessful owing to the large amounts of sample required and solubility issues. Therefore, we performed a wide spectrum of microscopy investigations on polyanion **1**, including SEM and AFM measurements.[29]

SEM investigations of solutions that were aged for approximately three weeks displayed agglomerates of circa 400 nm in diameter. As can be seen from the SEM/EDXS results (Figure 3a and Supporting Information, Figure S5), they consist of smaller aggregates that are 30–40 nm in size, and their elemental composition corresponds well to that of **1**

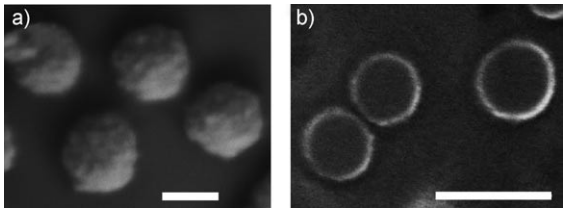

Figure 3. a) SEM and b) cryo-SEM investigations of aggregates generated from solutions of $[Gd_8As_{12}W_{124}O_{432}(H_2O)_{22}]^{60-}$ (scale bars: 200 nm).

in the solid state. Cryo-SEM investigations (Figure 3b) of solutions of **1** further indicate assembly into spherical clusters.

Concerning the stability of the entire $[Gd_8As_{12}W_{124}O_{432}(H_2O)_{22}]^{60-}$ polyanion **1** in solution, we conducted AFM investigations on solutions containing the $[Gd_8As_{12}W_{124}O_{432}(H_2O)_{22}]^{60-}$ ion a week after synthesis to circumvent any previous assembly processes in solution. The solution samples were immobilized on a mica substrate to achieve immediate insight into the solution behavior of the clusters. The results (for details, see the Supporting Information, Figure S6) clearly show that the POM forms bilayered hemispherical films on the substrate, with diameters in the range of 3 μm. Furthermore, burst agglomerates showed that they consist of two layers, each one circa 4 nm in height. This range corresponds with the length of $[Gd_8As_{12}W_{124}O_{432}(H_2O)_{22}]^{60-}$ (ca. 4.8 nm), such that the films might in principle be formed of two layers of intact polyanions.

The observed size of the clusters obtained using different microscopy techniques decreases in the order AFM > SEM > Cryo-SEM, and depends on the sample preparation method.

Whereas cluster diameters of up to 200 nm are obtained after the freeze-drying process for Cryo-SEM investigations, larger aggregates of circa 400 nm in size result from the air-dried conventional SEM samples. AFM measurements, however, show a quasi "in situ" scenario of hemispherical agglomerates with micrometer-scale diameters. Further DLS and SLS investigations aiming for the definite proof of the stability of polyanion (**1**) in solution are now in progress. They indicate a "blackberry" cluster formation (as indicated by the substructure of the aggregates in Figure 3a) that will be reported in due course.

Preliminary variable-temperature magnetic susceptibility data of polyanion **1** show that the χ_M versus T curve follows a Curie law from 5 K to 300 K and can be fitted for non-interacting Gd^{III} ions ($L=0$, $S=7/2$; see the Supporting Information, Figure S7). This result is in good agreement with the Gd–Gd distances of about 5.7 Å obtained from the crystal structure determination.

In summary, we have presented a versatile strategy for the construction of large POM architectures: The dilacunary $\{As_2W_{19}\}$ building block is efficiently linked by gadolinium(III) ions and templated by alkali cations to form a large discrete nanocluster. The novel polyanion $[Gd_8As_{12}W_{124}O_{432}(H_2O)_{22}]^{60-}$ (**1**) has been characterized in the solid state and its solution behavior is currently being investigated with different microscopy and light scattering techniques.

Our results represent a major step forward in the research on large polyoxotungstates on different fronts. First, $[Gd_8As_{12}W_{124}O_{432}(H_2O)_{22}]^{60-}$ (**1**) is the second-largest tungsten-containing cluster to date. Secondly, it is the first example of an octanuclear gadolinium-containing POM, thereby adding a new representative to the family of lanthanoid-containing polyoxometalates, with manifold potential applications. Gadolinium cations also act as efficient linkers to form large lanthanoid-containing POMs. Moreover, the terminal aqua ligands on the gadolinium centers can allow further derivatization reactions, which are expected to bring forward interesting compounds. All in all, this opens up new perspectives for the design of POM-based supramolecular functional materials and devices.

Experimental Section

$Na_{35}K_{14}Cs_{11}[Gd_8As_{12}W_{124}O_{432}(H_2O)_{22}]\cdot nH_2O$ ($n\approx123$): A sample of $K_{14}[As_2W_{19}O_{67}(H_2O)]$ (0.5262 g, 0.10 mmol), synthesized according to Kortz et al.[23c] was added under stirring to a solution of $Gd(NO_3)_3\cdot6H_2O$ (0.0903 g, 0.20 mmol) in 1M NaOAc/CH_3COOH (25 mL, pH 4.7). This solution was heated to 80 °C for 1 h and then filtered. Addition of 0.5M CsCl solution (0.50 mL) to the colorless filtrate, and slow evaporation at room temperature, led to a colorless crystalline product (block-shaped crystals) after about four to six weeks. Yield: 0.11 g (15%).

Crystal data for $Na_{35}K_{14}Cs_{11}[Gd_8As_{12}W_{124}O_{432}(H_2O)_{22}]\cdot nH_2O$ ($n\approx123$): A colorless crystal ($0.22\times0.18\times0.09$ mm^3) was mounted on a capillary tube for indexing and intensity data collection at 183(2) K on an Oxford Xcalibur Ruby CCD single-crystal diffractometer ($Mo_{K\alpha}$ radiation, $\lambda=0.71073$ Å). 60812 reflections collected ($2\theta_{max}=26.37$ (99.8% complete), 37477 unique ($R_{int}=0.080$), 16375 observed ($I>2\sigma(I)$). Routine Lorentz and polarization corrections were applied, and an absorption correction was performed using the ABSCALE 3 program.[30] Direct methods were used to locate the heavy metal atoms (SHELXS-97). The remaining atoms were located from successive Fourier maps (SHELXL-97).[31] Crystal data: $M_r=18016.97$, space group $P\bar{1}$, $a=19.5812(2)$, $b=28.0071(3)$, $c=29.9041(5)$ Å, $\alpha=66.2880(10)$, $\beta=82.9030(10)$, $\gamma=87.6960(10)°$, $V=14899.4(3)$ Å^3, $Z=2$, $\rho_{calcd}=4.016$ g cm^{-3}, $\mu=26.124$ mm^{-1}; $R_1=0.0677$, $wR_2=0.1743$ for $I>2\sigma(I)$, $R_1=0.1163$, $wR_2=0.1890$ for all data. Further details on the crystal structure investigations may be obtained from the Fachinformationszentrum Karlsruhe, 76344 Eggenstein-Leopoldshafen, Germany (fax: (+49) 7247-808-666; e-mail: crysdata@fiz-karlsruhe.de), on quoting the depository number CSD-420588.

IR data and elemental and thermogravimetric analyses are provided in the Supporting Information. Magnetization was measured in a Quantum Design DC-SQUID magnetometer (5.5 T-MPMS).

Atomic force microscopy (AFM) was performed on one week old samples of polyanion **1** with an Asylum MFP3D AFM in tapping mode. The cantilever used was a Mikromasch NSC-11 Ti-Pt oscillating at 121.7 kHz. A mica sheet was cleaved several times to obtain an atomically flat and clean surface, which was placed inside the liquid chamber. A freshly prepared as-synthesized solution of **1** kept for a week was slowly immobilized on the surface of the mica with the help of a microsyringe.

For scanning electron microscopy (SEM), performed on a Zeiss SUPRA 50 VP microscope, solution samples were deposited on a silicon wafer. The measurements were made without conductive coating at low voltage (1 kV) to minimize charging effects. Cryo-SEM measurements were performed on glow-discharged (15 nm) carbon-coated grids. A solution of **1** (ca. 3 μL) was applied to the surface of the treated carbon film for 60 s, and the remaining liquid was blotted off the grid with filter paper. The sample was then rapidly dipped into liquid nitrogen and subsequently transferred onto the cryo-stage from liquid nitrogen into the high vacuum cryo preparation device (BAF060) and freeze-dried for 1 h at −90 °C followed by −80 °C for 1 h. The freeze dried samples were then metal coated at −120 °C (2 nm W under 45° elevation angle and 2 nm with changing elevation angle from 0–90°). Coated samples were high vacuum cryo-transferred to the cryo-SEM and imaging was performed at −120 °C in a FE-SEM (Gemini 1530 equipped with a cryo-stage) at different acceleration voltages.

Received: June 18, 2009
Revised: August 11, 2009
Published online: October 27, 2009

Keywords: gadolinium · nanostructures · polyoxometalates · self-assembly · tungsten

[1] M. T. Pope, *Heteropoly and Isopoly Oxometalates*, Springer, Berlin, **1983**.
[2] M. T. Pope, A. Müller, *Angew. Chem.* **1991**, *103*, 56–70; *Angew. Chem. Int. Ed. Engl.* **1991**, *30*, 34–48.
[3] M. T. Pope, *Compr. Coord. Chem. II* **2003**, *4*, 635–678.
[4] C. L. Hill, *Compr. Coord. Chem. II* **2003**, *4*, 679–759.
[5] L. Cronin, *Compr. Coord. Chem. II* **2003**, *7*, 1–56.
[6] *Polyoxometalate Molecular Science* (Eds.: J. J. Borras-Almenar, E. Coronado, A. Müller, M. T. Pope), Kluwer, Dordrecht, **2004**.
[7] B. Hasenknopf, *Front. Biosci.* **2005**, *10*, 275–287.
[8] *Polyoxometalates: from Platonic Solids to Antiretroviral Activity* (Eds.: M. T. Pope, A. Müller), Kluwer, Dordrecht, **1994**.
[9] Special Issue on Polyoxometalates: *Chem. Rev.* (Ed.: C. L. Hill), **1998**, *98*, 1–389.
[10] *Polyoxometalate Chemistry: From Topology via Self-Assembly to Applications* (Eds.: M. T. Pope, A. Müller), Kluwer, Dordrecht, **2001**.

[11] *Polyoxometalate Chemistry for Nano-Composite Design* (Eds.: T. Yamase, M. T. Pope), Kluwer, Dordrecht, **2002**.
[12] J. Berzelius, *Poggendorff's Ann. Phys.* **1826**, *6*, 369.
[13] a) J. F. Keggin, *Nature* **1933**, *131*, 908 – 909; b) J. F. Keggin, *Proc. R. Soc. London Ser. A* **1934**, *144*, 75 – 77.
[14] C. L. Hill, C. M. Prosser-McCartha, *Coord. Chem. Rev.* **1995**, *143*, 407 – 455.
[15] J. Li, I. Huth, L. M. Chamoreau, B. Hasenknopf, E. Lacôte, S. Thorimbert, M. Malacria, *Angew. Chem.* **2009**, *121*, 2069 – 2072; *Angew. Chem. Int. Ed.* **2009**, *48*, 2035 – 2038.
[16] A. Dolbecq, J. D. Compain, P. Mialane, J. Marrot, F. Sécheresse, B. Keita, L. R. B. Holzle, F. Miserque, L. Nadjo, *Chem. Eur. J.* **2009**, *15*, 733 – 741.
[17] L. Zhongfeng, L. Weisheng, L. Xiaojing, P. Fengkui, L. Yingxia, L. Hao, *Magn. Reson. Imaging* **2007**, *25*, 412 – 417.
[18] R. D. Peacock, T. J. R. Weakley, *J. Chem. Soc A* **1971**, 1836 – 1839.
[19] a) *Gmelin Handbook of Inorganic Chemistry*, *Vol. B3a*, 8th ed., Molybdenum Suppl., **1987**, S. 339, and *Gmelin Handbook of Inorganic Chemistry*, *Vol. 836* **1989**, pp. 19 – 22; b) B. S. Bassil, M. H. Dickman, I. Römer, B. von der Kammer, U. Kortz, *Angew. Chem.* **2007**, *119*, 6305 – 6308; *Angew. Chem. Int. Ed.* **2007**, *46*, 6192 – 6195; c) R. C. Howell, F. G. Perez, S. Jain, W. D. Horrocks, Jr., A. L. Rheingold, L. C. Francesconi, *Angew. Chem.* **2001**, *113*, 4155 – 4158; *Angew. Chem. Int. Ed.* **2001**, *40*, 4031 – 4034; d) G. L. Xue, J. Vaissermann, P. Gouzerh, *J. Cluster Sci.* **2002**, *13*, 409 – 421; e) K. Fukaya, T. Yamase, *Angew. Chem.* **2003**, *115*, 678 – 682; *Angew. Chem. Int. Ed.* **2003**, *42*, 654 – 658; f) X. Fang, T. Anderson, C. Benelli, C. L. Hill, *Chem. Eur. J.* **2005**, *11*, 712 – 718; g) D. Drewes, M. Piepenbrink, B. Krebs, *Z. Anorg. Allg. Chem.* **2006**, *632*, 534 – 536; h) B. S. Bassil, M. H. Dickman, B. von der Kammer, U. Kortz, *Inorg. Chem.* **2007**, *46*, 2452 – 2458; i) C. Zhang, R. C. Howell, K. B. Scotland, F. G. Perez, L. Todaro, L. C. Francesconi, *Inorg. Chem.* **2004**, *43*, 7691 – 7701; j) F. Li, L. Xu, Y. Wei, G. Gao, L. Fan, Z. Li, *Inorg. Chim. Acta* **2006**, *359*, 3795 – 3799; k) P. Mialane, A. Dolbecq, J. Marrot, F. Sécheresse, *Inorg. Chem. Commun.* **2005**, *8*, 740 – 742; l) C. Schäffer, A. Merca, H. Bögge, A. M. Todea, M. L. Kistler, T. Liu, R. Thouvenot, P. Gouzerh, A. Müller, *Angew. Chem.* **2009**, *121*, 155 – 159; *Angew. Chem. Int. Ed.* **2009**, *48*, 149 – 153.
[20] K. Wassermann, M. H. Dickman, M. T. Pope, *Angew. Chem.* **1997**, *109*, 1513 – 1516; *Angew. Chem. Int. Ed. Engl.* **1997**, *36*, 1445 – 1448.
[21] U. Kortz, F. Hussain, M. Reicke, *Angew. Chem.* **2005**, *117*, 3839 – 3843; *Angew. Chem. Int. Ed.* **2005**, *44*, 3773 – 3777.
[22] A. Müller, S. Roy, *J. Mater. Chem.* **2005**, *15*, 4673 – 4677.
[23] a) C. Tourné, A. Revel, G. Tourné, M. Vendrell, *C. R. Seances Acad. Sci. Ser. C* **1973**, *277*, 643 – 645; b) C. Tourné, G. Tourné, *C. R. Seances Acad. Sci. Ser. C* **1975**, *281*, 933; c) U. Kortz, M. G. Savelieff, B. S. Bassil, M. H. Dickman, *Angew. Chem.* **2001**, *113*, 3488 – 3491; *Angew. Chem. Int. Ed.* **2001**, *40*, 3384 – 3386.
[24] F. Robert, M. Leyrie, G. Hervé, A. Tézé, Y. Jeannin, *Inorg. Chem.* **1980**, *19*, 1746 – 1752.
[25] a) F. Hussain, R. W. Gable, M. Speldrich, P. Kögerler, C. Boskovic, *Chem. Commun.* **2009**, 328 – 330; b) F. Hussain, B. Spingler, F. Conrad, M. Speldrich, P. Kögerler, C. Boskovic, G. R. Patzke, *Dalton Trans.* **2009**, 4423 – 4425.
[26] C. M. Tourné, G. F. Tourné, *J. Chem. Soc. Dalton Trans.* **1988**, 2411 – 2420.
[27] A. Tézé, M. Michelon, G. Hervé, *Inorg. Chem.* **1997**, *36*, 5666 – 5669.
[28] a) I. D. Brown, D. Altermatt, *Acta Crystallogr. Sect. B* **1985**, *41*, 244 – 247; b) A. Trzesowska, R. Kruszynski, T. J. Bartczak, *Acta Crystallogr. Sect. B* **2004**, *60*, 174 – 178.
[29] a) S. Kasas, A. Ikai, *Biophys. J.* **1995**, *68*, 1678 – 1689; b) M. J. Rosenbluth, W. A. Lam, D. A. Fletcher, *Biophys. J.* **2006**, *90*, 2994 – 3003.
[30] *CrysAlis Pro software system*, Version 171.32, Oxford Diffraction Ltd., Oxford, UK, **2007**.
[31] a) G. M. Sheldrick, *SHELXS-97*, A Program for the Solution of Crystal Structures, University of Göttingen, **1997**; b) G. M. Sheldrick, *SHELXL-97*, A Program for Crystal Structure Refinement, University of Göttingen, **1997**.

